Environmental Science and Pollution Research (2023) 30:111936–111946
https://doi.org/10.1007/s11356-023-30221-4

RESEARCH ARTICLE

Study on mechanical properties of coal gangue and fly ash mixture as backfill material based on fractal characteristics

Wei Li[1] · Lei Yue[1] · Yu Liu[1,2] · Shuncai Li[1,2] · Liqiang Ma[3] · Jintao Wang[1]

Received: 15 November 2022 / Accepted: 27 September 2023 / Published online: 11 October 2023

Abstract

Backfill mining can effectively alleviate the problems of surface collapse and ecological water pollution, in which the mechanical properties of backfill materials, including coal gangue and coal fly ash, have a decisive role in the effect of filling mining. In this study, we analyze the permeability characteristics of coal gangue filler through a set of homemade percolation test systems and introduce fractal characteristics to investigate the key factors affecting percolation in complex pores of broken coal gangue. The results indicate that the fractal dimensions of crushed coal gangue particles show an increasing trend with increasing axial loading and that the variation range is from 2.15647 to 2.58933. The coal fly ash concentration has a positive relationship with the acceleration factor. The permeability of crushed coal gangue follows a hierarchical distribution law and the permeability changes in the magnitude range of $10^{-11} \sim 10^{-9}$ m^2. The fractal dimension is inversely related to the permeability of crushed coal gangue. The experimental results show that the coal gangue will be further crushed and that adding a certain concentration of coal fly ash can achieve a better water barrier, which provides theoretical support and engineering significance for the stability analysis of geological engineering and backfill mining technology.

Keywords Backfill mining · Ecological water pollution · Crushed coal gangue · Geological engineering

Introduction

Coal mining has an indispensable role in the rapid economic development of China. Conversely, the solid waste generated by mining piles poses a series of threats to the surrounding environment. For instance, the massive accumulation of coal gangue waste causes a waste of land resources, while sulfide spillage or leaching in coal gangue will seriously pollute land resources and water resources (Yang et al. 2021; Ran et al. 2022; Wang et al. 2021). In addition, coal seam mining will cause a certain deformation fracture of the overburden during the mining process. As shown in Fig. 1, a large amount of groundwater will flow into the coal mining area when the fractures generated by the overburden fracture extend to the aquifer (Yan et al. 2021), causing secondary ecological environment damage, such as groundwater level drop and surface subsidence (Zhu et al. 2019).

To alleviate the ecological environmental problems caused by coal gangue accumulation and fracture of the water-bearing layer, backfill mining technology was proposed (Liu et al. 2021; Zhang and Cao 2021; Chen et al. 2022). Specifically, certain solid wastes, such as tailings, rock piles, and coal gangue, are selected as filling materials to backfill directly to the coal mine extraction area through filling equipment. The filling materials alleviate the fracture problem of the overlying water-bearing layer and subsequent series of hazards (Ding et al. 2016; Ma et al. 2020). However, the coal gangue filling material in the mined area may be repeatedly fractured due to the pressure of the overburden layer. Moreover, the strength and cementation of the backfill material may also be affected by the infiltration of water from the fracture of the water-bearing layer. Accordingly, studying the issues of load-bearing compression and hydraulic properties of fractured rock masses of filled bulk

Responsible Editor: Shimin Liu

✉ Yu Liu
pcl76277@163.com

[1] School of Mechanical Engineering, Jiangsu Normal University, Jiangsu, China

[2] State Key Laboratory of Coal Resources and Safety Mining, China University of Mining and Technology, Jiangsu, China

[3] School of Mines, China University of Mining and Technology, Jiangsu, China

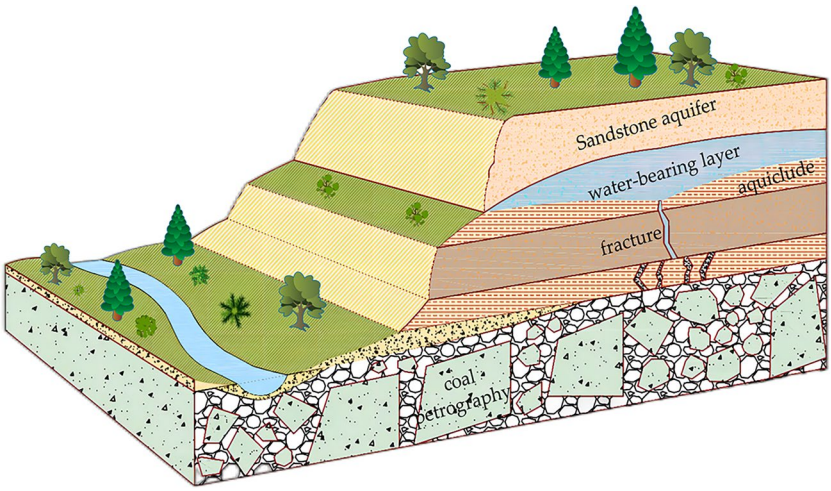

Fig. 1 Ecological harm caused by coal mining

materials in the compacted gateway will provide guidance to mining practitioners who use solid materials as backfill.

Scholars have conducted a set of studies on the load-bearing compressive properties of filling materials using numerical simulations, laboratory studies, and engineering practice. Yu et al. (2021) constructed irregular particle clusters by using particle element theory and PFC numerical simulation software, and found that the irregular particle morphology can more accurately reflect the permeability characteristics of small particles in collapse rock. Wang et al. (2014) utilized granular flow simulation software to study the compressive mechanical properties of coarse-grained soils and the stress–strain problems of gravel aggregates with different particle sizes, and obtained the degree of influence of cyclic loading on the compressive bearing. Yu et al. (2016) and Wang et al. (2016) conducted compression experiments on saturated crushed rock masses, crushed sandstone, and coal gangue with different grain size gradations, and obtained different cases of stress–strain exponential growth relationships and damage characteristics of compressive deformation. To better solve the actual engineering seepage collapse problem, the hydraulic properties of fractured rock masses were studied. After the famous Darcy law (Wahyudi et al. 2002) was proposed, conversely, it was determined that actual engineering did not conform to Darcy's law for fractured rock masses. The pressure gradient and seepage velocity have obvious nonlinear characteristics; hence, the non-Darcy law formula (Chen et al. 2015) was proposed by Forchheimer through numerous experimental studies. Since then, the research of scholars worldwide has rapidly developed in the field of seepage testing of fractured rock. Li et al. (2008) and Cao (2017) employed the transient permeability method to test the permeability of different coal samples and granite. It is found that the relationship between permeability and stress–strain and the air inclusions delay the attenuation of hydraulic pulse, which leads to the underestimation of permeability. Sinha et al. (2012) employed the steady-state method to obtain the permeability values of test samples by Darcy's formula. The results showed that the steady-state method was more accurate for accurately measuring the permeability of slightly compact specimens. Ma et al. (2018) and Lv et al. (2022) conducted tests with a homemade percolation experimental apparatus and discovered that the variation in permeability was directly related to the hydraulic gradient and the amount of filtered sand.

To analyze the compressive bearing of filling materials and the percolation of complex internal pores, the fractal dimension was introduced to characterize the degree of fragmentation of filling materials and spatial distribution characteristics, and a relationship with the permeability and other parameters was established. Yang et al. (2017) and Yu (2016) obtained the variable relationship among several physical parameters, such as the fractal dimension of multi-scale pores and tortuosity. Based on fractal geometry theory and techniques for laminar flow through tree-like branching networks with roughened channels, the relationships among pressure drops and permeability are investigated. Ma et al. (2019) established an improved model for predicting permeability evolution based on fractal dimension and determined that the loss of large particles and the change in fractal dimension were more significant at lower stress rates.

The researchers have explored the load-bearing compressive properties and hydraulic properties of these fill body materials through laboratory tests and numerical simulations, revealing insights for practical mining applications. However, there is a lack of in-depth investigation into the compressive and hydraulic properties of mixed fill materials with varying proportions. In this study, variations in the permeability coefficient and acceleration factor of crushed coal gangue specimens were mainly investigated using a

homemade percolation test system and fractal theory. The fractal characteristics of crushed coal gangue particles were also revealed.

Materials and methods

Preparation and proportioning of test materials

The filling materials selected for this test were coal gangue and coal fly ash samples. The tested coal gangue was collected from Xiaojihan Coal Mine in Yulin, Shanxi. X-ray diffraction spectra of coal gangue powder and fly ash were measured by X-ray powder diffractometer (model: D2 Advance), as shown in Fig. 2.

Coal gangue and fly ash are mostly composed of SiO2 and Al2O3, and the content of other components was slightly different. Large pieces of coal gangue were broken with the crusher; the four particle sizes required for the test were screened by a standard vibrating sieve and then mixed with different concentrations of coal fly ash. Among them, the particle size ranges of coal gangue are 2.5–5 mm, 5–8 mm, 8–12 mm, and 12–15 mm, as shown in Fig. 3.

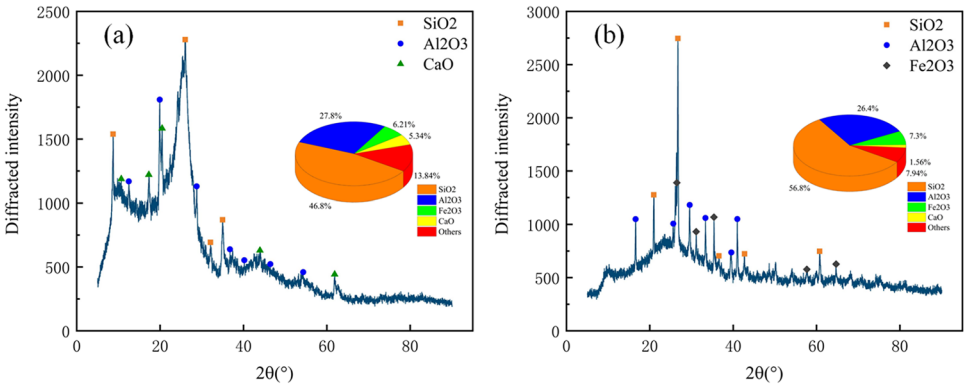

Fig. 2 The diffraction spectrum of samples and the content of main components: **a** coal gangue samples; **b** coal fly ash

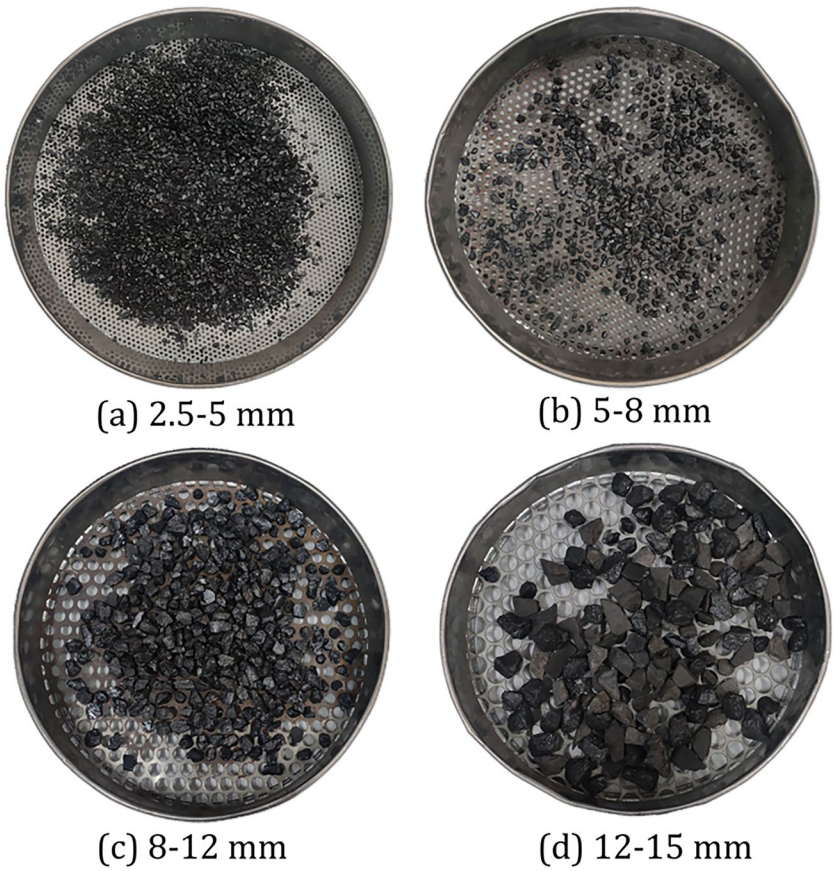

Fig. 3 Broken samples of different particle sizes

Test system and operating procedure

Through extensive experimentation and testing, the seepage test was conducted using an independently designed test system, as shown in Fig. 4. The system is mainly composed of a seepage instrument, an electronic tension–torsion testing machine, a flow meter, pressure sensors, an oil pump, a water tank, an acquisition card, and a computer. The seepage instrument is the core device of this test system. The upper tray (6) of the seepage instrument is fixed with bolts (7), and the lower tray is fixed and sealed with an O-shaped rubber seal (9) and bolts (4). The outside of the seepage instrument is the cylinder tube (1), and five pressure sensors are arranged on the left side of the cylinder tube to record the pressure data. Water flows upwards through the cylindrical tube via a barrel pipe (8) and flows out the device from a water pipe (3). The function of the flow piston (2) is to regulate the experimental flow rate, while the overflow groove cover (5) prevents water from escaping from the top. The electronic tension–torsion testing machine can provide a maximum axial load of 150 kN, and its model is WDD-LCJ-150. The water in the water tank can be injected from the bottom of the seepage instrument through the water pump. Flow meter and pressure sensors record data to the data acquisition card, which is subsequently processed by the computer for analysis of the stored experimental data.

Test protocol and procedure

The hydraulic and deformation tests of mixed samples of broken coal gangue and fly ash strictly followed the steps:

Step 1: The samples were prepared and mixed with fly ash according to the matching stages

The coal gangue was washed with water to remove the fine particles and soil left during the grading. The coal gangue can also be initially saturated. According to the volume of the cylinder, the mass of each group of samples was set to 1500 g. After removing 450 g of fly ash with a maximum mixing percentage of 30%, the remaining weight of coal gangue samples was graded. The sample quality of each particle size interval was matched according to Talbol Eq. (1) (Kong and Wang 2018). The mass distribution of each initial graded sample is shown in Table 1.

Table 1 Initial quality of crushing samples in different particle size intervals

Talbol power index *n*	Weight of each particle size (g)			
	2.5 ~ 5 mm	5 ~ 8 mm	8 ~ 12 mm	12 ~ 15 mm
0.2	733.77	192.18	78.22	45.83
0.4	512.78	303.78	143.78	89.66
0.6	358.34	361.75	198.33	131.58
0.8	250.42	384.60	243.32	171.66

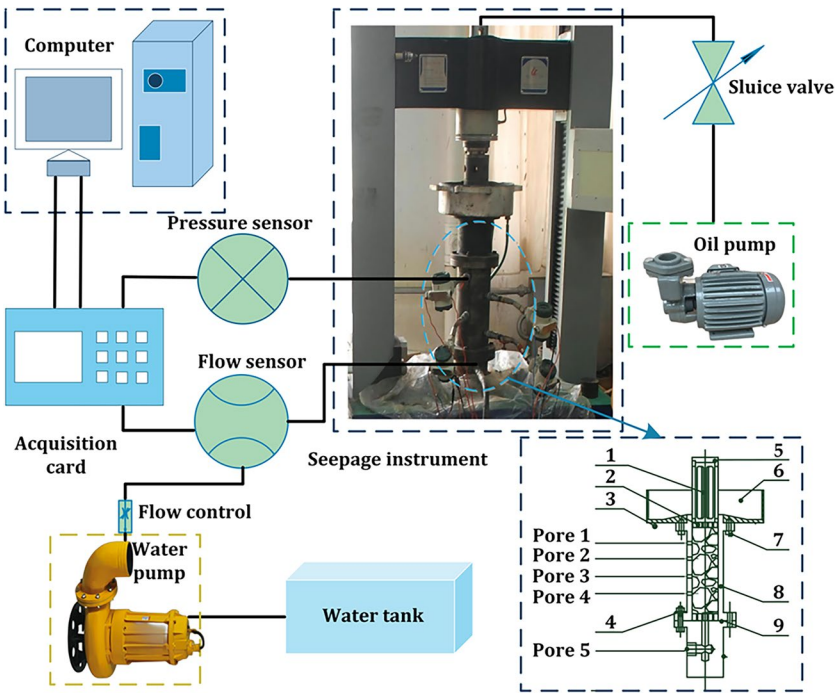

Fig. 4 Percolation experimental system

$$P = \left(\frac{d_r}{D_r}\right)^n \times 100\% \quad (1)$$

where P is the proportion of the mass of broken coal gangue with a diameter less than d_r and the total mass, d_r is the diameter of the broken coal gangue, D_r is the maximum diameter of the coal gangue, and n is the value of the Talbol power index.

The four graded coal gangue samples were mixed with 10%, 20%, and 30% fly ash, respectively, and left for 12 h at room temperature with ventilation.

Step 2: Conduct equipment assembly and sample preliminary processing

The mixed samples of coal gangue and fly ash were put into the cylindrical seepage vessel, and the whole seepage system was assembled. To eliminate the influence of the unsaturated state on the seepage test, the samples were saturated by low-pressure water injection until the flow rate was stable. Among them, the percolating fluid was water with mass density $\rho = 1000$ kg/m^3, dynamic viscosity $\mu = 1.01 \times 10^{-3}$ Pa·s, and coefficient of compressibility $C_f = 0.556 \times 10^{-9}$ Pa^{-1}. The experimental temperature (T) was 25 °C.

Step 3: Load axial stress and pass through different water pressure

In this step, the sample was first subjected to constant axial loadings, which were 40 kN, 60 kN, 80 kN, 80 kN, 100 kN, and 120 kN, each time a constant axial loading of 20 min, and then under an axial loading every 5 min into gradient water pressures. These were 1 MPa, 2 MPa, 3 MPa, and 4 MPa in sequence. The water pressure rose in a gradient over time and the changes between the four water pressures are synchronized. Each layer between the gradient changes is almost a horizontal line, as shown in Fig. 5.

Both a flow meter and a pressure sensor were used to record flow and pressure data. When the experiment was done, the sample was removed from the cylinder, and then particles of different particle sizes were selected with a standard vibrating screen. The samples were weighed and recorded with a high-precision electronic scale.

Principle of calculation of test parameters

According to the momentum equation, we employed the non-Darcy law formula of the porous medium (Zhang and Zhang 2019):

$$\rho c_a \frac{dV}{dt} = -\frac{\Delta p_i}{H} - \frac{\mu}{k} V - \rho \beta V^2 \quad (2)$$

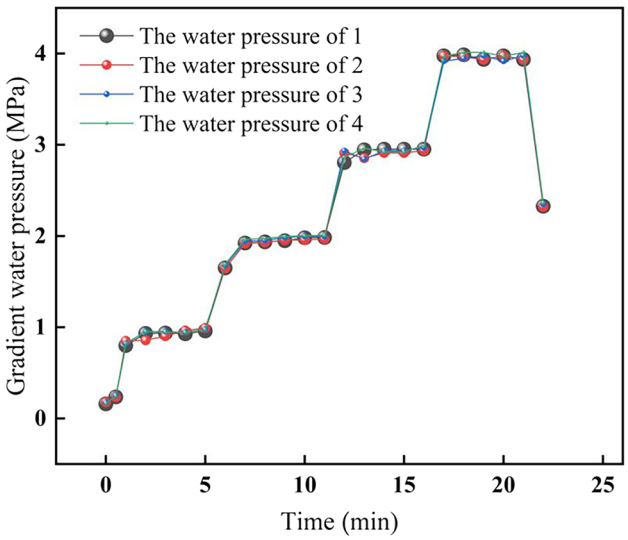

Fig. 5 Changes in water pressure over time

where $V = q/Q$, q is the flow rate at steady state, $Q = \pi\varphi^2/4$, φ is the inner diameter of the cylindrical tube, μ is the viscosity, ρ is the mass density of percolating fluid, Δp_i is the pore pressure difference, and H is the sample height.

According to previous studies of fractals (Li et al. 2019; Wu et al. 2021), the fractal dimension can be calculated:

$$\frac{M_d(x < d)}{M_t} = \frac{d^{3-D} - {d_{\min}}^{3-D}}{{d_{\max}}^{3-D} - {d_{\min}}^{3-D}} \quad (3)$$

where M_d is the particle mass with a particle size less than d; M_t is the sum of the particles; d is the particle size of the broken rock mass particle; d_{max} is the particle size of the largest particle; d_{min} is the particle size of the smallest particle; and D is the fractal dimension of the particle.

Under the action of axial loading in this test, the minimum particle size d_{min} is 0 compared with the larger particles in the sample, and the listing can then be expressed as:

$$\frac{M_d(x < d)}{M_t} = \left(\frac{d}{d_{\max}}\right)^{3-D} \quad (4)$$

Equation (4) takes the same log on both sides of the equation:

$$\lg\left(M_d/M_t\right) = (3 - D)\lg\left(d/d_{max}\right) \quad (5)$$

According to Eq. (5), a straight line is fitted in the double-log coordinate axis with a slope of *3-D*, and then the fractal dimension D of the broken coal gangue sample is obtained.

Results and discussion

Influence law of axial loading on fractal dimension

Different axial loadings have a certain influence on the fractal dimension of the broken coal gangue test samples, as shown in Fig. 6.

Figure 6 shows that the fractal dimension increases with increasing axial loading. The fractal dimensions of the three kinds of coal fly ash concentrations of the coal gangue specimens rapidly increase from 0 to 60 kN as the initially broken coal gangue large particle sample has the characteristics of the clear diamond and a small contact area. Hence, coal gangue specimens are very susceptible to fragmentation and cause a sharp increase in their fractal dimension under the action of axial loading. The fractal dimension rising trend slows with an increase in axial loading; when the particle is broken to a certain extent, increased contact between particles and particle migration is difficult. The broken coal gangue particles are fully in contact with each other and are further compacted. In addition, the change in the particle shape after fracture suppresses further fracture of the particles, and the close contact among the particles hinders their rearrangement. This is consistent with the findings by Wen et al. (2019): the overall deformation of the samples slowly increases, and the coal gangue samples rarely break. Consequently, the fractal dimension eventually gradually increases.

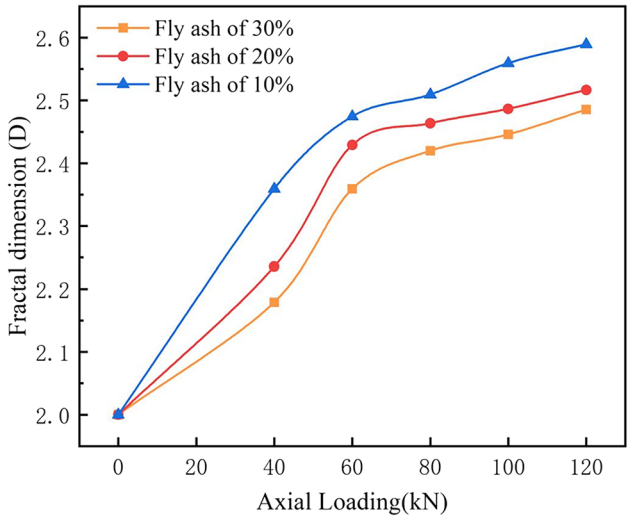

Fig. 6 Relations between axial loading and fractal dimension

Simultaneously, the fractal dimension decreases with increasing coal fly ash concentration under the same axial loading. With the same initial particle size classification and stress conditions, the concentration of coal fly ash directly affects the strength of the crushing sample. Broken particles are less likely as the concentration increases, leading to a further decrease in the fractal dimension.

Analysis of factors influencing the seepage acceleration coefficient

By increasing the axial loading, the seepage characteristics of non-Darcy flow are calculated according to the collected time series. Table 2 represents the flow rate and pressure data. The acceleration coefficient (C_a) changes of four different grain grading and three different coal fly ash concentrations are shown in Fig. 7.

It can be concluded that with the axial loading ranging from 40 to 80 kN, the acceleration coefficient is constantly increasing. This is consistent with the findings of Kan et al. (2021); it should be noted that when the axial loading is greater than 80 kN, the acceleration coefficient decreases and then has a small recovery. The internal structure of the coal gangue test sample is destroyed with increasing axial

Table 2 Seepage characteristics of the coal gangue sample test

Serial number	Axial loading (kN)	Talbol power index n	Coal fly ash concentration	Non-Darcy seepage characteristics		
				k/m^2	β/m^{-1}	Ca
1	40	0.2	10%	2.07×10^{-9}	3.26×10^{9}	4.56×10^{5}
2	80		20%	8.96×10^{-10}	-3.84×10^{12}	1.33×10^{9}
3	120		30%	2.45×10^{-11}	1.54×10^{13}	8.96×10^{9}
4	40	0.4	10%	2.98×10^{-9}	5.78×10^{9}	6.87×10^{5}
5	80		20%	6.43×10^{-10}	8.86×10^{11}	1.15×10^{8}
6	120		30%	5.76×10^{-11}	-3.84×10^{12}	1.48×10^{9}
7	40	0.6	10%	3.56×10^{-9}	4.98×10^{9}	3.43×10^{5}
8	80		20%	2.04×10^{-10}	-3.45×10^{10}	5.87×10^{7}
9	120		30%	8.32×10^{-11}	1.34×10^{11}	2.34×10^{8}
10	40	0.8	10%	4.19×10^{-9}	1.13×10^{9}	3.80×10^{5}
11	80		20%	1.72×10^{-9}	9.10×10^{10}	8.07×10^{6}
12	120		30%	9.26×10^{-10}	-5.67×10^{10}	1.14×10^{7}

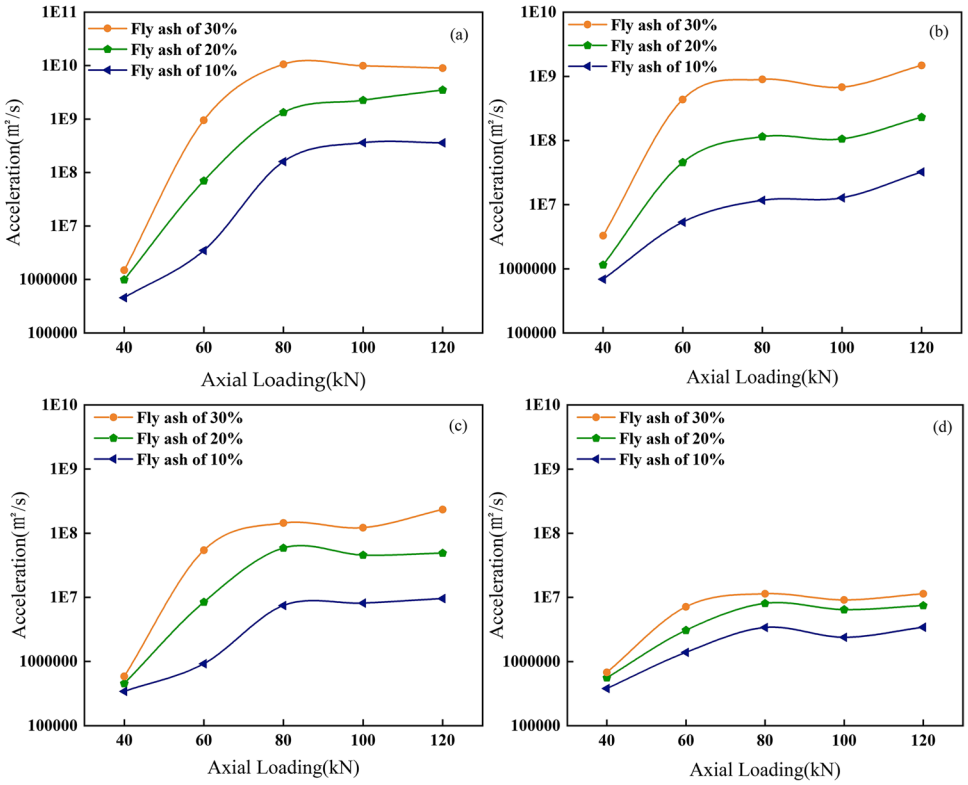

Fig. 7 Change pattern of the acceleration coefficient (C_a) under different axial loadings: **a** Talbol power index 0.2; **b** Talbol power index 0.4; **c** Talbol power index 0.6; **d** Talbol power index 0.8

loading. The pores do not continue to increase, and the permeability exhibits a slight increase. Moreover, after the axial loading exceeds 100 kN, the acceleration coefficient slowly changes as the coal gangue test sample is basically in the full compaction state, and slide movement between two subtle particles produces slow changes in the acceleration coefficient.

Through a comparison of four sizes of coal gangue samples, the acceleration coefficient decreases with an increase in the broken sample size. The acceleration coefficient reflects the change process of the fluid viscosity force; when a large coal gangue sample enters the water pressure, the fluid viscosity force exhibits a small change. On the other hand, the acceleration coefficient is inversely proportional to the porosity of the broken coal gangue sample. The acceleration coefficient decreases as the Talbol power index increases. Different concentrations of coal fly ash for the acceleration coefficient also have a certain influence, as shown in Fig. 6. The acceleration coefficient is proportional to the coal fly ash concentration. The degree of cementation of broken coal gangue is greater with increasing coal fly ash concentration, which further causes an increase in the acceleration coefficient.

Permeability evolution pattern

Analogous to the change process of the gradient water pressure, the tube height is divided into four layers to analyze the compaction samples of different layers. By processing the sample data of different layers separately, the change rule of four-layer permeability is obtained.

Figure 8 shows the permeability trend diagram of the Talbol power index is 0.4 and coal fly ash concentrations of 20% as an example. Notably, the top half of the diagram depicts a thumbnail of the sample, and the bottom half of the diagram depicts the different degrees of compaction inside the sample. The specimen will have particularly obvious transition zones at the beginning of the seepage. The permeability in the transition zone substantially varies. The seepage flow is extremely unstable, and with increasing axial loading, the permeability of broken coal gangue samples will be reduced.

The least squares method is a statistical method for fitting data or estimating parameters. Its fundamental principle involves the search for one or more curves that minimize the sum of squared vertical distances between observed data points and corresponding points on these curves. Based on test data and Eq. (2), permeability was fitted using the least squares method and the objective function is obtained as follows:

$$f(i) = \rho c_a dx(i) - \frac{\mu v(i)}{k} + \beta \rho v(i) - dp(i) \tag{6}$$

The permeability k, the non-Darcy factor β, and acceleration coefficient Ca can be obtained by Eq. (6).

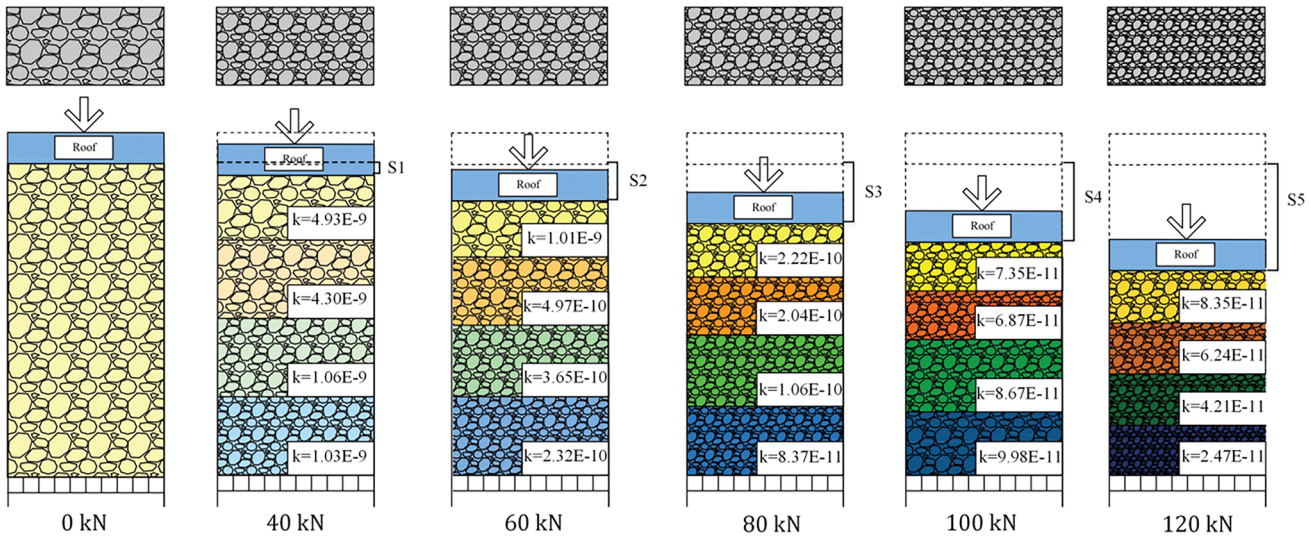

Fig. 8 Trend diagram of the permeability of each layer under different axial loadings

Figure 9 shows the measured values and fitted curves of permeability changes of each layer; the change curves of permeability of each layer are basically the same. Under the same axial loading, the permeability of the test sample decreases layer by layer when the axial pressure increases to 100 kN. Figure 9d shows that the original configuration of the broken coal gangue test sample is destroyed, and the conductivity of the coal gangue test samples increases. If the pore pressure does not continue to increase, the penetration rate slightly recovers. Different from the conclusion of Feng et al. (2018), there was no significant change in the permeability after the axial loading exceeded 100 kN. When the sensitivity of the permeability to axial loading decreases, coal gangue particles squeeze against each other, and the sliding

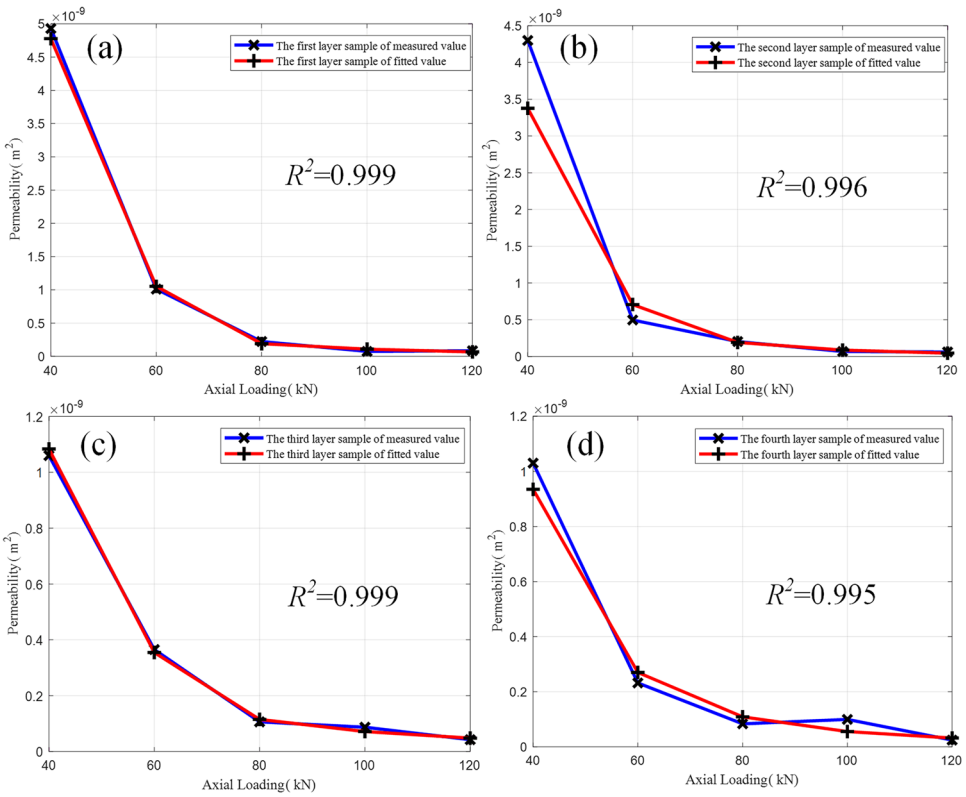

Fig. 9 Permeability of four layers varies with different axial loadings: **a** first layer sample; **b** second layer sample; **c** third layer sample; **d** fourth layer sample

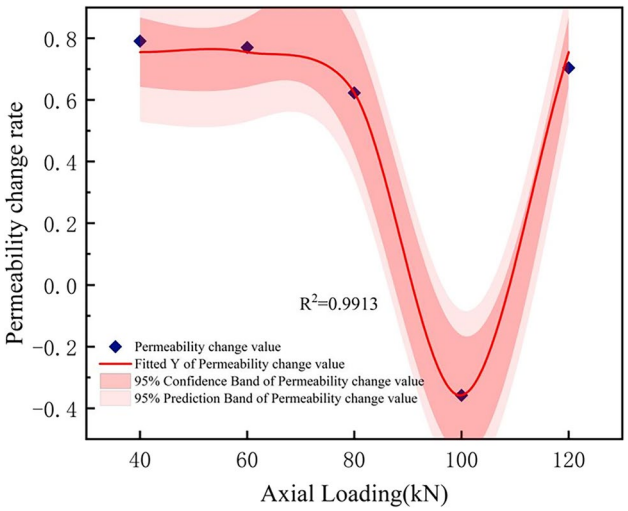

Fig. 10 Relationship between permeability change rate and axial loading

deformation eventually reaches the equilibrium state. The axial loading continuously reduces the porosity of the broken coal gangue samples, the particles are more uniform, and the permeability varies by two orders from 10^{-11} to 10^{-9} m^2.

The results in Fig. 10 show that the rate of change of seepage rate decreases steadily with the axial loading firstly. When the axial loading is 100 kN, the rate of change of permeability is small and conforms to the fitted exponential function with an accuracy of 0.9913. As can be seen from the 95% confidence band, the change rate of permeability is included in it, and the change range is relatively large. At this time, the change rate of permeability ranges from –0.5 to 0.1. This is because the sample tends to be tightly compacted and the permeability does not change significantly, which is consistent with the permeability of the above four layers. Therefore, it is concluded that the broken coal gangue test sample has a strong deformation ability and can be used as a backfill mining material to prevent water failure caused by surface settlement and fracture of the water-bearing layer. The results of the influence of particle size grade on hydraulic performance were compared by Ma et al. (2021). The permeability value of the four samples when the compressive stress is greater than 4 MPa is less than 10 μm^2, and the permeability decline rate is fast from 0 to 3 MPa, which is basically consistent with the permeability change in the early stage of this paper. Different from the investigated permeability method, the layered permeability method adopted in this paper can more directly obtain the internal connection between permeability and porosity and compaction state. The results show that adding a certain concentration of coal fly ash can improve the adhesion degree of the test sample of broken coal gangue to effectively control the mining settlement and protect the ecological environment.

Variation pattern of permeability and fractal dimension

Based on the mass of different particle sizes before and after the compaction of the broken coal gangue samples, the relationship between fractal dimension and permeability is obtained, as shown in Fig. 11.

The fractal dimension and permeability are fitted into a primary equation, and the specific equation expression is shown above, where the fractal dimension ranges from 2.15647 to 2.58933. Zhang et al. (2020) obtained the results of increasing the fractal dimension from 2.38 to 2.56 in the 95% humidity test, which is basically consistent with the results of this paper. However, different from the change in humidity, this paper explores the effect of fractal dimension on permeability by changing the coal fly ash concentration. The effect of fractal dimension on permeability was investigated by changing the coal fly ash concentration. The results show that permeability gradually decreases with increasing fractal dimension. As the fractal dimension increases, the fragmentation of the coal gangue specimen intensifies, resulting in an increase in the number of small particles produced. Consequently, this leads to a direct increase in the number of pores in the broken specimen. The average diameter of pores and pore volume are inversely proportional. At this time, the small particles of the coal gangue sample under axial loading are continuously displaced and compacted, and particle size distribution recombination causes pore blockage by small particles, which leads to a permeability decrease.

Conclusions

In this study, the basic mechanical properties of mixed specimens of coal gangue (obtained from a single mine source) and coal fly ash under different axial loading

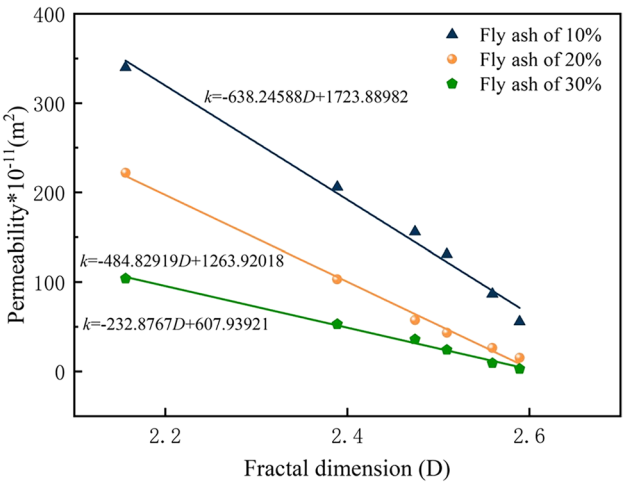

Fig. 11 Relation for permeability and fractal dimension

conditions were tested using a homemade percolation test system. The variance ratio of permeability between different axial loading levels and the relationship between axial loading and acceleration coefficient under different grain grading were obtained. The characteristic relationships between axial loading and permeability and particle fractal dimension for different coal fly ash concentrations were discussed. The following conclusions are made based on the experimental results.

(1) The increasing rate of fractal dimension further increases when the axial loading ranges from 0 to 60 kN and decreases when the axial loading is greater than 60 kN. This rate is negatively correlated with the coal fly ash concentration, and in this study, the increasing range of fractal dimension is 2.15647 ~ 2.58933.
(2) The axial loading and acceleration coefficients are positively proportional, and the grain grading of the crushed coal gangue specimen is inversely proportional to the acceleration. The higher the concentration of coal fly ash for the same stress and particle size, the greater the acceleration coefficient of the crushed specimen. The non-Darcy flow β factor changes in the range of $10^9 \sim 10^{12}$ m^{-1}, and the acceleration factor Ca changes in the range of $10^5 \sim 10^9$. The results show that the crushed coal gangue specimen is mixed under a smaller grain grading, and a higher coal fly ash concentration as filler material will yield better performance.
(3) The water pressure rises in a gradient with creep time and is basically in a synchronized state as the axial loading reaches a preset value while maintaining a constant load to the corresponding creep time. This finding is helpful for the correctness and reliability of parameters such as permeability and fractal dimension. Porosity is a physical parameter that directly affects the permeability of crushed specimens, while the permeability varies with each layer of specimen; the magnitude range of permeability k is $10^{-11} \sim 10^{-9}$ m^2. The results indicate that the specimens in the compaction process undergo asynchronous crushing and particle sliding displacement, which is directly related to the height of the test barrel diameter.
(4) According to the correspondence between permeability and particle fractal dimension, it was determined that the broken coal gangue specimens have obvious fractal characteristics. It is suggested to compress the broken coal gangue specimens with axial loading at a lower rate to reduce the risk of overburden and avoid the destruction of water-bearing layers.

Abbreviations Symbols

P: The proportion of the mass of broken coal gangue with diameter less than d_r and the total mass; d_r: The sieve hole diameter; D_r: The maximum scale of the particle; n: The value of the Talbol power index; V: The seepage velocity; q: The flow rate at steady state; Q: $\pi\varphi^2/4$, φ Is the inner diameter of the cylindrical tube; μ: The viscosity; ρ: The mass density of percolating fluid; Δp_i: The pore pressure difference; H: The sample height; k: The permeability; β: The non-Darcy factor; Ca: Acceleration coefficient; M_d: The particle mass with a particle size less than d; M_t: The sum of the particles; d: The particle size of the broken rock mass particle; d_{max}: The particle size of the largest particle; d_{min}: The particle size of the smallest particle; D: The fractal dimension of the particle

Acknowledgements The work was supported by the Postgraduate Research & Practice Innovation Program of Jiangsu Province, No.KYCX22_2843.

Author contribution Wei Li: conceptualization, writing—review and editing. Yu Liu: methodology, resources, supervision. Yue Lei: validation, visualization, data curation. Shuncai Li: formal analysis. Liqiang Ma: investigation. Jintao Wang: software. All the authors have read and agreed to the published version of the manuscript.

Funding This research was funded by the Research Fund of The State Key Laboratory of Coal Resources and safe Mining, grant numbers SKLCRSM18KF009 and SKLCRSM19KF013, and the National Natural Science Foundation of China under grant number 52034007.

Data availability All data are contained within the paper, and a report of any other data is not included.

Declarations

Ethics approval and consent to participate Not applicable.

Consent for publication Not applicable.

Competing interests The authors declare no competing interests.

References

Cao C (2017) Transient surface permeability test: experimental results and numerical interpretation. Constr Build Mater 138:496–507. https://doi.org/10.1016/j.conbuildmat.2017.02.024

Chen YF, Liu MM, Hu SH, Zhou CB (2015) Non-Darcy's law-based analytical models for data interpretation of high-pressure packer tests in fractured rocks. Eng Geol 199:91–106. https://doi.org/10.1016/j.enggeo.2015.10.011

Chen Q, Tao Y, Zhang Q, Qi C (2022) The rheological, mechanical and heavy metal leaching properties of cemented paste backfill under the influence of anionic polyacrylamide. Chemosphere 286:131630. https://doi.org/10.1016/j.chemosphere.2021.131630

Ding QL, Ju F, Song SB, Yu BY, Ma D (2016) An experimental study of fractured sandstone permeability after high-temperature

treatment under different confining pressures. J Nat Gas Sci Eng 34:55–63. https://doi.org/10.1016/j.jngse.2016.06.034
Feng M, Wu J, Ma D, Ni X, Yu B, Chen Z (2018) Experimental investigation on the seepage property of saturated broken red sandstone of continuous gradation. Bull Eng Geol Env 77:1167–1178
Kan Z, Zhang L, Li M, Yuan X, Huang M (2021) Investigation of seepage law in broken coal and rock mass under different loading and unloading cycles. Geofluids 2021:1–14
Kong H, Wang L (2018) The mass loss behavior of fractured rock in seepage process: the development and application of a new seepage experimental system. Adv Civ Eng 2018:1–12. https://doi.org/10.1155/2018/7891914
Li S, Zhang T, Chen Z (2008) Penetration test of high gas coal. Coal Field Geol Explor 36(4):11–14
Li L, Wu W, El Naggar MH, Mei G, Liang R (2019) Characterization of a jointed rock mass based on fractal geometry theory. Bull Eng Geol Env 78(8):6101–6110. https://doi.org/10.1007/s10064-019-01526-x
Liu Y, Liu J, Yang B, Yuan S (2021) Assessing water and sand inrushes hazard reductions due to backfill mining by combining GIS and entropy methods. Mine Water Environ 40(4):956–969. https://doi.org/10.1007/s10230-021-00829-4
Lv A, Bahaaddini M, Masoumi H, Roshan H (2022) The combined effect of fractures and mineral content on coal hydromechanical response. Bull Eng Geol Env 81(5):1–20. https://doi.org/10.1007/s10064-022-02669-0
Ma D, Cai X, Zhou Z, Li X (2018) Experimental Investigation on hydraulic properties of granular sandstone and mudstone mixtures. Geofluids 2018:1–13. https://doi.org/10.1155/2018/9216578
Ma D, Duan H, Liu J, Li X, Zhou Z (2019) The role of gangue on the mitigation of mining-induced hazards and environmental pollution: an experimental investigation. Sci Total Environ 664:436–448. https://doi.org/10.1016/j.scitotenv.2019.02.059
Ma D, Duan H, Liu W, Ma X, Tao M (2020) Water–sediment two-phase flow inrush hazard in rock fractures of overburden strata during coal mining. Mine Water Environ 39(2):308–319. https://doi.org/10.1007/s10230-020-00687-6
Ma D, Zhang J, Duan H, Huang Y, Li M, Sun Q, Zhou N (2021) Reutilization of gangue wastes in underground backfilling mining: overburden aquifer protection. Chemosphere 264:128400. https://doi.org/10.1016/j.chemosphere.2020.128400
Ran H, Guo Y, Feng G, Li C (2022) Failure properties and stability monitoring of strip and column cemented gangue backfill bodies under uniaxial compression in constructional backfill mining. Environ Sci Pollut Res 1–16. https://doi.org/10.21203/rs.3.rs-1120748/v1
Sinha S, Braun EM, Passey QR, Leonardi SA, Wood III AC, Zirkle T, Boros JA, Kudva RA (2012) Advances in measurement standards and flow properties measurements for tight rocks such as shales. Eur Unconv Resour Conf cp-285–00034. https://doi.org/10.3997/2214-4609-pdb.285.spe152257
Wahyudi I, Montillet A, Khalifa AA (2002) Darcy and post-Darcy flows within different sands. J Hydraul Res 40(4):519–525. https://doi.org/10.1080/00221680209499893
Wang P, Liu J, Li X, Fang J (2014) Study on static shear characteristics of gravel aggregate under biaxial compression. J Rail 36(06):87–92
Wang W, Li H, Xiong Z, Su Y, Zhang P (2016) Study on compaction deformation of paired gangue. J Undergr Space Eng 12(06):1553–1558
Wang X, Liu Y, Li L, Yenusah CO, Xiao Y, Chen L (2021) Multi-scale phase-field modeling of layer-by-layer powder compact densification during solid-state direct metal laser sintering. Mater Des 203:109615. https://doi.org/10.1016/j.matdes.2021.109615
Wen L, Luo ZQ, Qin YG, Luo ZY (2019) The use of Hoek Brown failure criterion on determination of the geo-mechanical parameters of a grouting consolidation body. IEEE Access 7:142703–142714
Wu J, Yin Q, Gao Y, Meng B, Jing H (2021) Particle size distribution of aggregates effects on mesoscopic structural evolution of cemented waste rock backfill. Environ Sci Pollut Res 28(13):16589–16601. https://doi.org/10.1007/s11356-020-11779-9
Yan Y, Huang Q, Xie Y, Liu T, Xu Q, Fan F, Wang Y (2021) Failure analysis of urban open-cut utility tunnel under ground fissures environment in Xi'an, China. Eng Fail Anal 127:105529. https://doi.org/10.1016/j.engfailanal.2021.105529
Yang S, Fu H, Yu B (2017) Fractal analysis of flow resistance in tree-like branching networks with roughened microchannels. Fractals 25(01):1750008. https://doi.org/10.1142/S0218348X17500086
Yang K, Zhao X, Wei Z, Zhang J (2021) Development overview of paste backfill technology in China's coal mines: a review. Environ Sci Pollut Res 1–13. https://doi.org/10.1007/s11356-021-16940-6
Yu B (2016) Porous media fractal theory and methods with percolation mechanics. Summary collection of the 9th National Academic Conference on Fluid mechanics 221
Yu B, Chen Z, Wu J (2016) Study on compression deformation and fractal characteristics of graded saturated crushed rock. J Min Saf Eng 33(02):342–347
Yu K, Zheng C, Ren F (2021) Numerical experimental study on ore dilution in sublevel caving mining. Min Metall Explor 38(1):457–469. https://doi.org/10.1007/s42461-020-00337-z
Zhang Y, Cao S (2021) Control of water-flowing fracture development with solid backfill mining: designing a backfill body compression ratio for water resources protection. Mine Water Environ 40(4):877–890. https://doi.org/10.1007/s10230-021-00821-y
Zhang C, Zhang L (2019) Permeability characteristics of broken coal and rock under cyclic loading and unloading. Nat Resour Res 28(3):1055–1069. https://doi.org/10.1007/s11053-018-9436-x
Zhang T, Guo Y, Pang M, Peng W, Yang L, Zhang S (2020) Study on creep fractal characteristics of pressure crushed coal rock under different environmental humidity. J Min Saf Eng 37(5):1037–1044
Zhu X, Guo G, Liu H, Chen T, Yang X (2019) Experimental research on strata movement characteristics of backfill–strip mining using similar material modeling. Bull Eng Geol Env 78(4):2151–2167. https://doi.org/10.1007/s10064-018-1301-y